The Meteoritical Society

Meteoritics & Planetary Science 43, Nr 7, 1099–1111 (2008)
Abstract available online at http://meteoritics.org

Molecular study of insoluble organic matter in Kainsaz CO3 carbonaceous chondrite: Comparison with CI and CM IOM

Laurent REMUSAT[1‡], Corentin Le GUILLOU[2], Jean-Noël ROUZAUD[2], Laurent BINET[3], Sylvie DERENNE[1*], and François ROBERT[4]

[1]Laboratoire de Chimie Bioorganique et Organique Physique, UMR CNRS 7618 BioEMCo, Ecole Nationale Supérieure de Chimie de Paris, 11 rue Pierre et Marie Curie, 75005 Paris, France
[‡]Present address: Laboratoire de Géologie des Systèmes Volcaniques, UMR CNRS 7154, Institut de Physique du Globe de Paris/Université Pierre et Marie Curie, 4 place Jussieu, 75005 Paris, France
[2]Laboratoire de Géologie, UMR CNRS 8538, Ecole Normale Supérieure, 24 rue Lhomond, 75231 Paris Cedex 5, France
[3]Laboratoire de Chimie de la Matière Condensée de Paris, UMR CNRS 7574, Ecole Nationale Supérieure de Chimie de Paris, 11 rue Pierre et Marie Curie, 75005 Paris, France
[4]Laboratoire d'Etude de la Matière Extraterrestre, UMS CNRS 2679 NanoAnalyses, Museum National d'Histoire Naturelle, 61 rue Buffon, 75005 Paris, France
[*]Corresponding author. E-mail: sylvie-derenne@enscp.fr

(Received 25 May 2007; revision accepted 28 August 2007)

Abstract–Kainsaz CO3 insoluble organic matter (IOM) was studied using Curie point pyrolysis, electronic paramagnetic resonance (EPR), and high-resolution transmission electron microscopy (HRTEM) to determine the effect of thermal metamorphism on molecular chondritic fingerprints. Pyrolysis released a very low amount of products that consist of one- and two-ring aromatic units with methyl, dimethyl, and ethyl substituents. Moreover, Kainsaz IOM contains two orders of magnitude fewer radicals than Orgueil, Murchison, and Tagish Lake IOM. In addition, no diradicaloids were found in Kainsaz, although they are thought to constitute a specific signature for weakly organized extraterrestrial organic compounds in contrast to terrestrial ones. HRTEM reveals a very heterogeneous structure, with microporous disordered carbon, mesoporous graphitic carbons and graphite. Graphitization likely occurs and explains the differences between Kainsaz and CI or CM IOM. Heating stress experienced by Kainsaz IOM, on the parent body and/or prior its accretion, is likely responsible for the differences in molecular and structural organizations compared with those of CI and CM IOM.

INTRODUCTION

Carbonaceous chondrites are among the most studied objects from the solar system because of their primitive bulk compositions, noble gases concentration and composition, and occurrence of primitive condensates and organic compounds. These organics can be recovered as soluble compounds and, predominantly, as a macromolecular insoluble fraction, hereafter named insoluble organic matter (IOM). Organics have been so far almost exclusively studied in CI and CM carbonaceous chondrites due to high abundance (for a review, see Pizzarello et al. 2006). The combination of results from pyrolysis (Levy et al. 1973; Sephton et al. 2000, 2004; Remusat et al. 2005a), chemical degradation (Hayatsu et al. 1980; Remusat et al. 2005b), and solid-state nuclear magnetic resonance (Gardinier et al. 2000; Cody and Alexander 2005) allowed the determination of key features of the molecular structure of IOM from CI and CM chondrites. It is now admitted that the IOM constitutes of rather small aromatic units, highly cross-linked with short, branched aliphatic chains. Oxygen atoms are located in ether or ester linkages between aromatic units. In contrast, nitrogen atoms are involved into aromatic structures as pyrroles. These features are consistent with recent high-resolution transmission electron microscopy (HRTEM) observations performed on Orgueil and Murchison IOM (Derenne et al. 2005). Indeed, HRTEM is an efficient tool to study organic samples at the nanometer scale (Papoular et al. 1996; Galvez et al. 2002; Le Guillou et al. 2007); it was extensively used to characterize coals, chars, and soots (Boulmier et al. 1982; Rouzaud and Oberlin 1990; Beyssac et al. 2002), Precambrian organic matter (Jehlicka and Rouzaud 1993; Westall et al. 2006) and IOM of various carbonaceous chondrites including Allende, Orgueil, and Murchison

(Daulton et al. 1996; Harris et al. 2000; Garvie and Buseck 2004). HRTEM clearly shows that Orgueil and Murchison IOMs are poorly organized and constitute of aromatic units with an average size of 2–3 aromatic rings in diameter, and that the aromatic units are smaller than PAHs observed in the interstellar medium, which could be the result of a selective preservation of small PAHs in the IOM before their destruction by UV radiation (Derenne et al. 2005).

Electronic paramagnetic resonance (EPR) is a powerful method to determine the occurrence of radicals in natural samples and their distribution. For instance, it allowed the determination of radical concentration in organic matter of Precambrian chert, which is highly refractory (Gourier et al. 2004). EPR has also successfully determined a typical behavior for chondritic IOM through the study of Orgueil, Murchison, and Tagish Lake IOM (Binet et al. 2002, 2004a, 2004b). It clearly shows that these disordered IOM share two common signatures that discern these organic samples from terrestrial ones: the occurrence of abundant diradicaloid moieties—i.e., aromatic moieties with two unpaired electron radicals that can be stabilized by delocalization of electrons over the aromatic rings—and a heterogeneous distribution of organic radicals. These two features are interpreted as the fingerprint of an interstellar-like process involved in the organosynthesis of extraterrestrial organic matter.

Along with isotopic data, these features are used to describe the origin and evolution of the organic matter of the most primitive object of the solar system. It is not simple to determine a scenario for the story of the IOM, as it could be the result of several processes taking place in the interstellar medium, the protosolar nebula, and the parent bodies of the carbonaceous chondrites. To distinguish the contribution of these processes, it is essential to study the variability between several classes of carbonaceous chondrites. Indeed, carbonaceous chondrites are divided into different classes that represent different stages of thermal metamorphisms and aqueous alterations (Scott and Krot 2003). As described before, most of the previous studies on organic contents in carbonaceous chondrites have focused on CI and CM, i.e., the most aqueously and the least thermally altered carbonaceous chondrites.

Kainsaz is a member of the Ornans type (i.e., CO) carbonaceous chondrites, which constitute a metamorphic series analogous to that seen in ordinary chondrites (McSween 1977). Several studies have dealt with the determination of the petrographic type by using various proxies as mineralogical associations (Scott and Jones 1990; Chizmadia et al. 2002), noble gas and presolar grain content (Newton et al. 1992a; Huss et al. 2002), organic matter structure, or isotope ratios (Greenwood and Franchi 2004; Bonal et al. 2007 and references therein). These studies revealed that Kainsaz has a moderate to intermediate metamorphic grade (3.2 to 3.6) depending on the technique used. Organic matter is supposed to have kept the overprint of thermal stress on the parent body, assuming a common organic precursor. Nevertheless, the modifications at the molecular level induced by this stress are not well assessed.

We applied some methods used on CI and CM IOM to study the molecular structure of Kainsaz (CO3) IOM. Little is known about molecular structure of IOM from CO chondrites compared to data available on CI and CM chondrites. Bonal et al. (2007) have reported Raman spectra showing that organics in Kainsaz, and especially IOM, reveal a higher degree of organization than CI and CM. Indeed, the spectra are characteristic of weakly graphitized carbons (important defect band at about 1350 cm^{-1}), which is consistent with noticeable thermal stress since the D band is not so broad (FWHM = 117 cm^{-1}) compared to Orgueil and Murchison IOM.

In the present study, we used pyrolysis, HRTEM, and EPR to characterize the IOM of Kainsaz meteorite and we compare the obtained data with those from CI and CM IOM. Our goal was to asses the effect, at the molecular level, of a thermal stress on carbonaceous chondrites parent bodies. Furthermore, our purpose was to examine if Kainsaz IOM would exhibit the same EPR signatures as Orgueil, Murchison, and Tagish Lake IOM.

EXPERIMENTAL

Sample Preparation

Kainsaz fell in Russia (Tatarstan republic) in 1937. About 9 g of Kainsaz were provided by the Museum National d'Histoire Naturelle of Paris, France. The sample was crushed in an agate mortar and IOM was subsequently isolated as described in Remusat et al. (2005b). In brief, the ground sample was subjected to several extractions in water (stirring under reflux for 48 h), acetone (stirring at room temperature for 2 h twice) and dichloromethane/methanol (2:1, v/v, stirring at room temperature for 2 h twice). The solid residue was then subjected to HF/HCl treatment: it was successively stirred in HCl (6N) for 24 h at room temperature, in a mixture of HF/HCl (28N/6N, 2:1, v/v) for 24 h at room temperature under nitrogen flux and finally in HCl (6N) for 4 h at 60 °C. The acid residue was then extracted with acetone and a mixture of CH_2Cl_2/MeOH, 2:1, v/v and was dried under N_2. Carbon and hydrogen contents were determined by the SGS laboratory in Evry, France.

The acid residue represents about 1.4 wt% of the ground Kainsaz meteorite and contains 30.5 wt% and 0.4 wt% of carbon and hydrogen, respectively (H/C atomic ratio: 0.16). It also contains over 50.4 wt% of inorganic material that likely constitutes of oxides and/or sulfides. These values are consistent with previous data (Newton et al. 1992b) and with a content of 0.63 wt% of carbon in the bulk sample reported by Semjonova et al. (1982).

Curie Point Pyrolysis

Flash pyrolysis was performed using tubular ferromagnetic wires with a Curie temperature of 650 °C. Pyrolysis was produced by inductive heating, using a high-frequency generator (Fisher 0316M), of the wires to their Curie temperature in 0.15 s (and holding for 10 s); about 5 mg of sample was loaded in wires. The pyrolysis device was directly coupled to a gas chromatograph-mass spectrometer (GCMS) (Hewlett Packard HP-5890 gas chromatograph and Hewlett Packard HP-5889A series II mass spectrometer, electron energy 70 eV, ion source temperature 220 °C, scanning from 40 to 650 a.m.u., 0,7 scan/s). Helium was used as carrier gas. A fused silica capillary column coated with chemically bound Restek RTX-5MS (30 m × 0.25 mm i.d., 0.5 μm film) was used to separate the pyrolysis products. After a 10 min period at 50 °C, the GC oven was programmed from 50 °C to 300 °C at 4 °C/min.

EPR

EPR experiments were carried out as previously described by Binet et al. (2002, 2004a) with a Bruker Elexsys E500 spectrometer operating at 9.4 GHz equipped with a SHQ resonator and a helium flow ESR900 cryostat from Oxford Instruments for temperature variations from 4 K to room temperature. The spin concentration was estimated by comparison of the EPR intensity of the sample with of a standard diphenylpicrylhydrazyl (DPPH) sample with a known spin concentration.

HRTEM

HRTEM was carried out using a Jeol 2011 microscope, operating at 200 kV at the TEM facilities of Sciences Faculty of University Pierre et Marie Curie of Paris, France. When hkl planes are quasi-parallel to the incident electron beam (i.e., under the Bragg angle) and separated by at least 0.14 nm (the resolution of this microscope), fringes appear due to interference between the transmission electron beam and hkl diffracted beams and are representative of the profile of the hkl planes. In the IOM, the profile of the polyaromatic structure can be directly imaged (Rouzaud and Oberlin 1990; Galvez et al. 2002; Rouzaud and Clinard 2002).

The sample was finely crushed into an agate mortar under alcohol. A droplet of the obtained suspension was deposited on a lacey carbon grid and dried. Only very thin particles (>10 nm if possible) and placed across the web of the lacey grid were imaged, in order to avoid artefacts due to the quasi-amorphous carbon-supporting film.

Image analyses were conducted in a similar way as described by Derenne et al. (2005). In brief, quantitative structural and microtextural data are obtained after skeletonization of selected HRTEM images (Rouzaud and Clinard 2002). A 16 × 16 nm^2 area is digitalized on 1024 × 1024 pixels with a resolution of 4000 ppi, each pixel corresponding to 0.1725 nm. The image is processed by specific software that reduces the noise background by filtration at the Fourier transform level. After thresholding, a binary image is obtained and represents a skeleton of carbon layers profile. This skeleton is further analyzed with several criteria taken in account: (1) all shorter fringes than an aromatic ring (i.e., 0.246 nm) are eliminated, since without physical sense; (2) the C–C bond being 0.142 nm, a fringe crossed by segments smaller than this value are considered as rectilinear; (3) two fringes spaced by more than 0.7 nm are considered as non-stacked layers as van der Waals interactions between graphene layers are supposed to be negligible at this distance. Using this method, the length of all the fringes, L, i.e., the extent of the aromatic layers, was individually measured, by considering that a layer could be curved until a distortion ratio arbitrarily fixed at 40%. As is classically done with X-ray diffraction, coherent domains are defined by the parts of the polyaromatic planes that are involved in the stacking of parallel planes (within a 15° margin). They are characterized by their diameter La and height Lc along with the number N of stacked layers and interlayer spacings d (Galvez et al. 2002; Rouzaud and Clinard 2002).

RESULTS

Pyrolysis

Figure 1 represents the chromatogram of the 650 °C Curie point pyrolysis coupled with GC-MS of Kainsaz IOM. Pyrolysis released only minor amount of products. This is likely the result of the thermal stress that is supposed to have affected the CO chondrites parent bodies. The poor diversity of products detected is also striking when compared with the released products from pyrolysis of CM and CI IOM (Remusat et al. 2005a). Indeed, in these IOMs (Fig. 1), a diverse and complete series of aromatic compounds, from one to four aromatic rings with methyl and ethyl substitutions, along with series of phenols (O-bearing aromatic compounds) and thiophenes (S-containing heteroatomic aromatic compounds) are detected upon Curie point pyrolysis. All these compounds exhibit a complete structural diversity with all possible isomers detected without any predominance.

In Kainsaz IOM, only toluene, dimethyl- and ethyl-benzenes, C_3-benzenes, and naphthalene are detected, the latter being the most abundant aromatic product. As stressed above, aromatic hydrocarbons are classical compounds detected from pyrolysis of chondritic IOM (e.g., Shimoyama 1997; Sephton et al. 2000; Remusat et al. 2005a) and are related to the aromatic nature of the IOM. This observation is consistent with previous pyrolysis at 740 °C of CO3 Antarctic

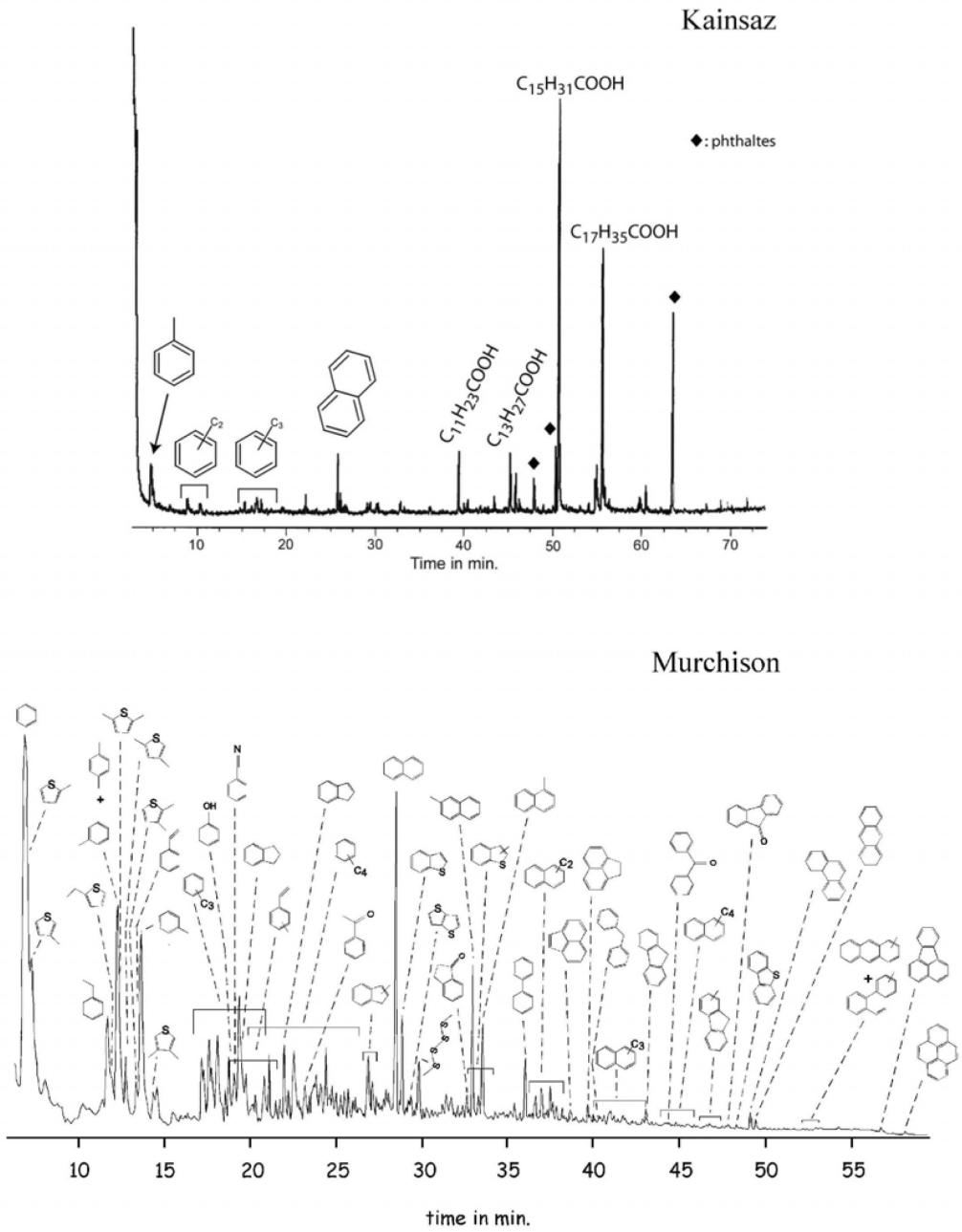

Fig. 1. 650 °C Curie point pyrochromatogram of Kainsaz IOM. The carboxylic acids and the phthalates are likely contaminants, while aromatic hydrocarbons seem to be indigenous released products. For comparison, 650 °C Curie point pyrochromatogram of Murchison IOM is also reported (from Remusat et al. 2005a).

meteorites, which released the same aromatic compounds (Murae 1995). Semjonova et al. (1982) have detected several organic compounds, for instance phenanthrene, perylene, and coronene, released from the heating under vacuum of bulk samples of Kainsaz. But these compounds are mainly high molecular weight polycyclic aromatic hydrocarbons (PAHs) that cannot be detected under the present analytical conditions. Moreover, these heating experiments were long (52 h), that should have enhanced the formation of larger PAHs through annealing of smaller units. Furthermore, these experiments were conducted on bulk samples and interactions with mineral matrix could result in different release pattern upon pyrolysis, due to possible catalytic processes.

The detection of only a few PAHs as indigenous pyrolysis products is consistent with the very low H/C atomic ratio: about 0.16 for Kainsaz IOM relative to 0.75 for Orgueil and Murchison IOM (high H/C ratios are signatures of aliphatic moieties, while low H/C of aromatic units; for example, H/C = 0.5 in coronene). A decrease in H/C is commonly associated with an increase in aromaticity.

Moreover, larger aromatic units are more thermally refractory and so pyrolysis only releases very few products.

The most abundant products are fatty acids ranging from C_{12} to C_{18} with a strong even-over-odd predominance. This distribution is highly similar to that encountered in biological samples and so must be related to terrestrial contamination of the sample. As several solvent extractions were done on our sample prior to pyrolysis, contaminants must be intimately associated with IOM. These acids were already released upon pyrolysis with TMAH of the Orgueil meteorite (Remusat et al. 2005a) and were interpreted as the possible result of terrestrial bacteria growth since the fall of the meteorite on Earth. Since Kainsaz has stayed over 70 years on Earth, such process can also be considered, even if the sample was collected and kept in a meteorite collection. Moreover, contamination during sample handling cannot be ruled out. The phthalates observed in the pyrolysis trace must not be taken into account, as these are typical contaminants from the laboratory environment and particularly from plastics used for sample handling and acid demineralization.

EPR Experiments

Figure 2a shows the EPR spectrum of Kainsaz IOM recorded at room temperature over an extended field range. A broad signal at $g \approx 2.25$, corresponding to $B_0 \approx 300$ mT, and with peak-to-peak linewidth ≈130 mT is observed. This signal most probably arises from ferromagnetic acid resistant minerals like iron/chromium oxides or sulfides. Indeed, such oxides/sulfides were also identified using HRTEM (see below). Figure 2b shows the EPR spectrum of Kainsaz IOM recorded at room temperature over a restricted field range about 335 mT. The baseline deviation is actually due to the broad signal of the ferromagnetic residues. A narrow signal is observed at magnetic field $B_0 = 335.26$ mT and with peak-to-peak linewidth ≈1 mT. This signal corresponds to carbonaceous radicals in the IOM and exhibits major differences as compared to the signal of the radicals in the Orgueil, Murchison and Tagish Lake meteorites. First, the *g* value of these radicals, $g = 2.0024–2.0026$, is significantly lower than the *g* values of the radicals in Orgueil, Murchison, and Tagish Lake meteorites, which are in the range of 2.0030–2.0032 (Binet et al. 2004b). The deviation of the *g* value from the free electron value $g_e = 2.0023$ is due to the spin-orbit interaction experienced by the unpaired electrons of the radicals. Therefore, as shown by EPR investigations on terrestrial IOM such as coals (Retcofsky et al. 1968), this interaction in carbonaceous radicals is enhanced when the wave functions of the unpaired electrons are delocalized over heteroelements, so that the deviation increases when the heteroelement content increases. Among the most common heteroelements, oxygen and nitrogen, oxygen has a stronger effect due to its stronger intrinsic spin-orbit interaction. From the data of Retcofsky et al., *g* values above 2.0030 as

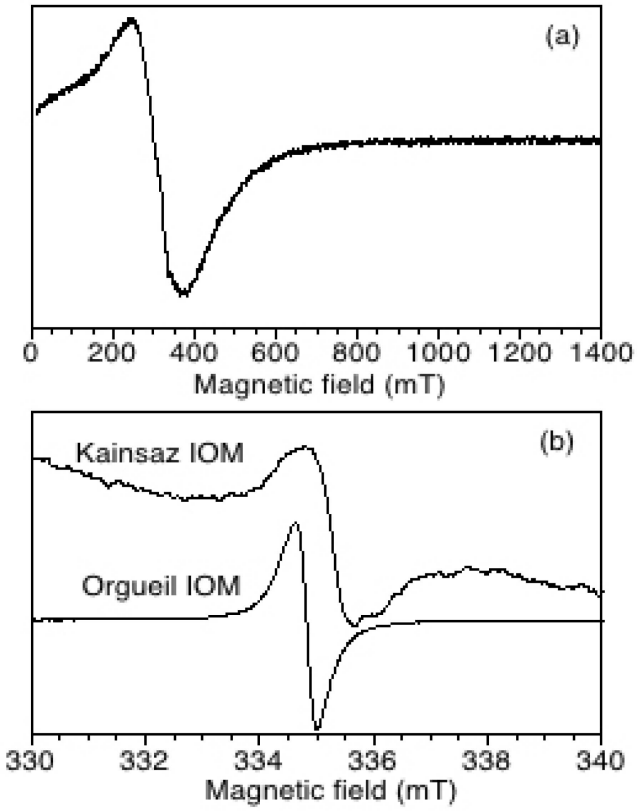

Fig. 2. a) Room temperature EPR spectrum of Kainsaz IOM over an extended field range, showing the resonance of magnetic mineral residues mixed with the IOM. b) Room temperature spectra over a restricted range about 335 mT of Kainsaz and Orgueil IOMs, showing the resonance of the carbonaceous radicals in the IOMs. Please note that the amplitudes of the spectra in (b) are not at the same scale.

measured for the Orgueil, Murchison and Tagish Lake meteorites are obtained for O/C > 0.1. This is consistent with the O/C values for the IOMs of these meteorites, which are in the of range 0.15–0.22. On the other side, the lowest values $g = 2.0027$ among the data of Retcofsky et al. correspond to O/C = 0.02–0.05. In the case of the radicals in Kainsaz meteorite, the *g* value is even lower and is identical to the value measured for radicals in amorphous heteroelement-free carbon (Barklie 2001). This shows that the radicals in Kainsaz do not contain any heteroelements.

The second difference with the IOMs of the Orgueil, Murchison, and Tagish Lake meteorites concerns the spin concentration at 300 K, which was determined and compared with those of Orgueil, Murchison, and Tagish Lake (see Table 1). The spin concentration in Kainsaz IOM appears to be about two orders of magnitude lower than in primitive carbonaceous chondrites and 3 orders of magnitude lower than terrestrial kerogens (Binet et al. 2002).

The third difference is the absence in Kainsaz IOM of moieties with thermally accessible triplet states, which were reported in the IOM of Orgueil and Murchison (Binet et al.

Table 1. Spin concentration at 300 K in IOM from Kainsaz, Orgueil, Murchison, and Tagish Lake.

	Spin concentration (10^{16} g^{-1})	References
Kainsaz (CO3)	8.0 ± 5	This study
Orgueil (CI)	700 ± 80	Binet et al. 2002
Murchison (CM)	180 ± 30	Binet et al. 2002
Tagish Lake (C2?)	1800 ± 600	Binet et al. 2004b

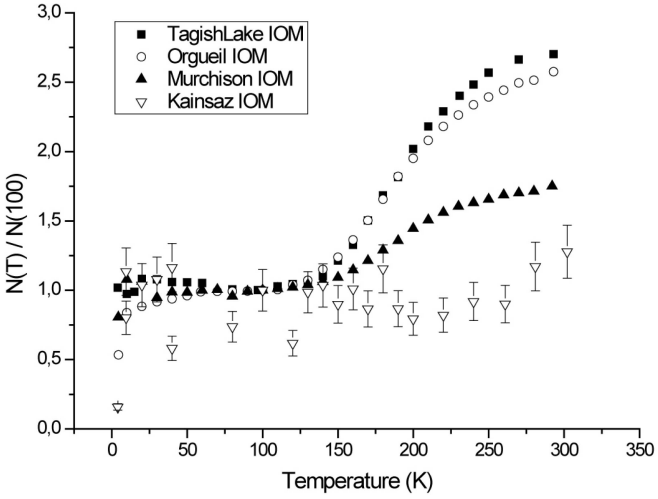

Fig. 3. Temperature dependence of the spin concentration normalized to the value at 100 K for the Kainsaz IOM. For comparison, the temperature dependence of the normalized spin concentration for Orgueil, Murchison, and Tagish Lake IOMs (from Binet et al. 2004b) is also plotted.

2004a) and of Tagish Lake (Binet et al. 2004b). In the latter three meteorites, these moieties, which accounted for 24 to 40% of the total radicals, manifested themselves in EPR by an increase in spin concentration when the temperature is increased above 150 K (Fig. 3). This original feature, unobserved in terrestrial IOM, was attributed to the occurrence of diradicaloids (Binet et al. 2004a). In contrast, the spin concentration in Kainsaz IOM is independent of temperature (Fig. 3), indicating that Kainsaz IOM contains no diradicaloids.

HRTEM Observations

At first glance, when compared with Orgueil and Murchison IOM, HRTEM observations of Kainsaz IOM reveal a very heterogeneous multi-scale organization showing particles with different structures: triperiodic (graphite sensu stricto: Fig. 4a), partially triperiodic (highly graphitized folded lamella: Fig. 4b), biperiodic (turbostratic porous particles: 4c–4e) and with different microtextures (i.e., nanostructures), lamellar: 4a and 4b, microporous: 4f, mesoporous: 4c, 4d, and 4e. Graphite or highly graphitized particles appear as folded lamellae; in the folds, the polyaromatic layers are on the Bragg angle and can be imaged. The layers are large (several tens of nanometers) and well stacked (N can reach several tens), and their interlaying spacing being low (closed to 0.3354 nm, the interlayer spacing of true graphite). In this case, such IOM organization is a fingerprint of a high degree of maturation. Nevertheless, not all the areas exhibit such organization. In most of the areas observed, the carbon exhibits poor organization: the layers are nanometer-sized, usually wrinkled, the number N of stacked layers is usually only 2 to 5, and d the interlayer spacing is larger than 0.35 nm. Such disordered carbons usually show porous microtexture; microporous when the pore size is smaller than 2 nm (see Fig. 4f) and mesoporous when it is between 2 and 50 nm (Fig. 4c, 4d, and 4e). In contrast, CI and CM IOMs exhibit a noticeably lower order with only porous disordered carbons with micropores but no clearly visible mesopores like those observed in Kainsaz.

In some places, IOM shows globule-like shells (Fig. 4e). Interestingly, Nakamura et al. (2002, 2006) have recently described hollow organic nanoglobules in Tagish Lake matrix. These kinds of structures were also reported in CM chondrites (Garvie and Buseck 2004). But these objects have a diameter between 140 nm and 1700 nm and appear rather amorphous, whereas the diameter of Kainsaz organic spheres is only about 40 nm and the wall is clearly made of nanometer-sized polyaromatic structures. Consequently, it seems unlikely that the organic spheres observed in Kainsaz IOM are related to the hollow organic globules in Tagish Lake matrix. Moreover, in some places, some iron/chromium oxides/sulfides grains (as detected by energy dispersive X-ray spectroscopy (EDS) occur embedded into polyaromatic carbon layers (Fig. 4f); these grains have rather the same diameter as the globule spheres, i.e., 40 nm. It seems likely that the globules are remnant templates of oxide grains lost during sample preparation. As the oxides/sulfides might constitute the major acid resistant minerals in the sample, representing about 50 wt% of the acid residue, it is consistent to observe such figures in several places. By looking in detail at the relations between those grains and the carbon layers, it looks like a carbon coating, i.e., a template (Fig. 5); the aromatic layers are parallel to the external shape of the grains. This association is sometimes not obvious (see, for example, Fig. 4f) since the layers need to be in the Bragg angle to be observed. The same kind of association was also reported by Nakamura et al. (2002) in Tagish Lake IOM, aside from hollow globules. These inorganic grains might then predate the association of organics and silicates resulting in the formation of the parent body of Kainsaz chondrites. This

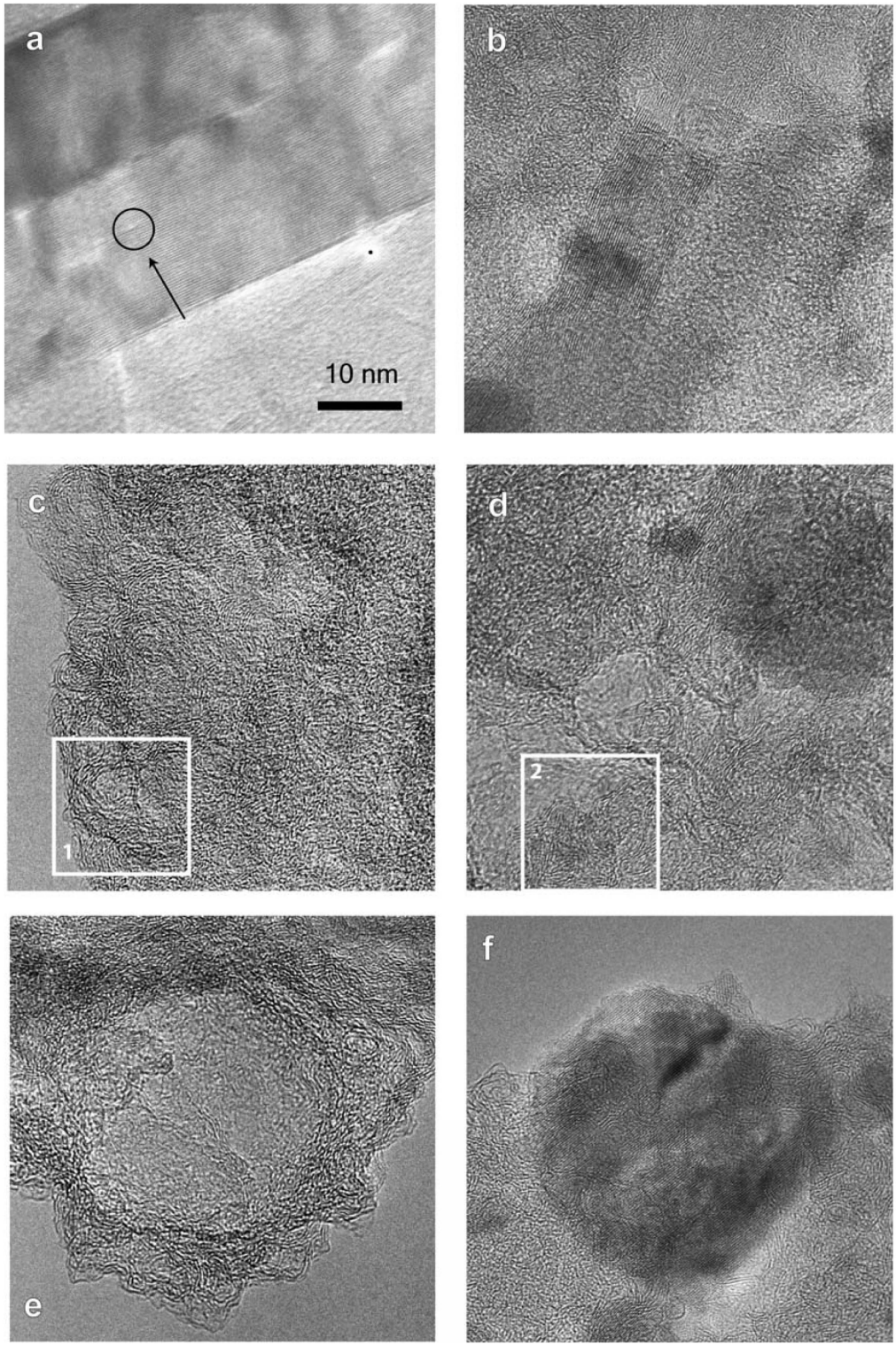

Fig. 4. HRTEM pictures of Kainsaz IOM. All pictures were taken at 400 kX magnification. Each picture represents a square of 50 nm × 50 nm. a) Highly graphitized carbon, with long straight plans and high number of stacked layers; the interlayer spacing is closed to that of graphite; note the presence of some dislocations (dark circle). b) Disordered graphitic carbon showing numerous defects responsible for slightly wrinkled layers. c) and d) Graphitic mesoporous carbons; a mesopore is clearly visible in the center on the square in (c) and above the white square in (d). e) Carbon "nanoglobule" (or rather a mesoporous carbon shell resulting from the coating of a mineral grain), which may be due to the loss of an oxide/sulfide grain (f) during grid preparation. The white squares 1 and 2 show two typical areas studied by image analysis (Table 2).

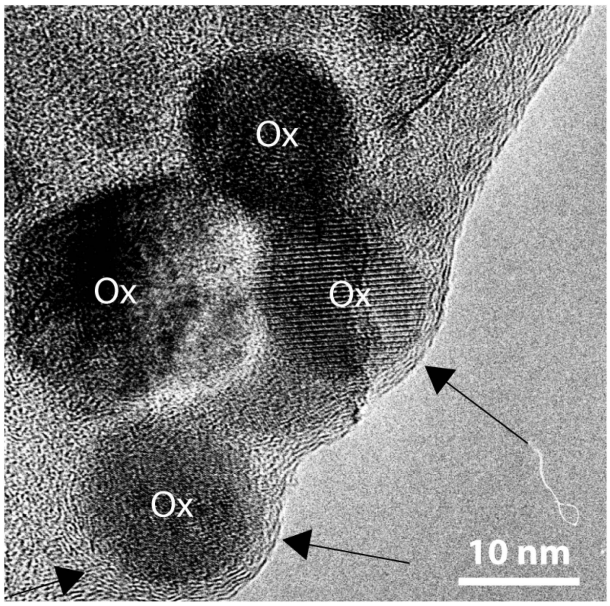

Fig. 5. HRTEM picture of Kainsaz IOM showing several oxide grains (Ox) embedded into organic material. The black arrows show that aromatic layers are surrounding the grains following their shape indicating that the grains were trapped into the IOM while it was synthesized.

association is not an artefact of sample demineralization, and it shows how such tiny oxides/sulfides grains are associated to IOM into the matrix of Kainsaz. Interestingly, small primitive SiO_2 grains (less than 1 μm) have been found embedded into the IOM of Murchison meteorites (Aléon et al. 2005). The smaller oxides/sulfides grains we found embedded into Kainsaz IOM could also be very primitive grains trapped in the early solar system. Indeed, iron sulfides have been observed in circumstellar disk (Keller et al. 2002). This topic is beyond the scope of this study and would need additional experiments to be assessed.

Figure 6 shows microtextural (i.e., nanostructural) features as nanoporosity that could be related to onion-like nanostructures (multi-layered rings 5–10 nm in diameter). As discussed later, these structures might be the remnants of nanodiamonds transformed in graphitic carbons upon heating (Le Guillou and Rouzaud 2007).

Image analysis on weakly organized areas was also undertaken in order to obtain at least semi-quantitative structural data on these kinds of carbon that represent almost 70% of the whole sample (visual estimation). We have calculated distributions of layer length, interlayer spacing and number of stacked layers from several scanned images recorded on several locations in the sample. Average parameters are reported in Table 2, along with data from Orgueil, Murchison, and Tagish Lake IOM study (Derenne et al. 2005). The distributions of average parameters from a dozen of areas are reported in Fig. 7. Two representative regions are indicated in Fig. 4 in squares 1 and 2.

The lengths of the continuous layers range from 0.25 to 1.25 nm (i.e., 1 to 5 rings large), with a mean value of 0.50 nm. When compared to Orgueil and Murchison distributions, those for Kainsaz are quite close, which seems to be in contrast with visual observation showing a noticeably better organization for Kainsaz. Indeed, pictures should reflect a higher layer length for Kainsaz. However, the human eye, binding layers of which are aligned and tight, overestimates the length: it tends to connect discontinuous aligned fringes so they appear longer. By contrast, distortions of the layers are responsible of tilts of the layers according to the incident beam; consequently the Bragg conditions are no longer completely filled and such interference error induces variations in the grey level distribution. Depending on the value given to the threshold, distorted (but probably continuous) fringes characterized by variable grey levels can appear "cut" in the skeletonized image. In fact, when the fringes are observed in details in the raw image, it appears that the continuity of the layers can be interrupted by variations in the grey level; this is especially visible in the case of graphite lamellae (see the top left corner of the image in Fig. 4a), but can also occur in more disordered carbons. The thresholding step is the most sensitive one during skeletonization process. If the layer interruption is tight, then it might be erased, but if it is too wide, then the program would cut the layer into two parts, drastically reducing its length. However, the proportion of non-stacked layers is in agreement with visual estimation: 60% in Kainsaz; lower than in Orgueil and Murchison IOM (Table 2).

The number of stacked layers in coherent domains in Kainsaz is close to that of Tagish Lake, Orgueil, and Murchison (Table 2). The distribution of this number (Fig. 7) is not obviously different from that of Orgueil and Murchison. When looked into detail, it appears that Kainsaz contains a larger proportion of higher domains, i.e., made of a significantly larger number of stacked layers. More differences rise when interlayer spacing is considered. The average measured value is about 0.40 nm, significantly smaller than in Tagish Lake, Orgueil, and Murchison. The peak in the distribution of interlayer spacing of Kainsaz IOM (Fig. 7) shifts to low values, indicating that layers are better stacked than in Orgueil and Murchison.

DISCUSSION

Comparison between Kainsaz IOM and Samples from CI and CM

Pyrolysis clearly demonstrates that Kainsaz IOM lacks thermally labile organic matter (OM) and heteroatomic functional groups, whereas CI and CM IOM contain pyrroles, ester and ether linkages (Hayatsu et al. 1980; Remusat et al. 2005a). Sephton et al. (2003) have determined three

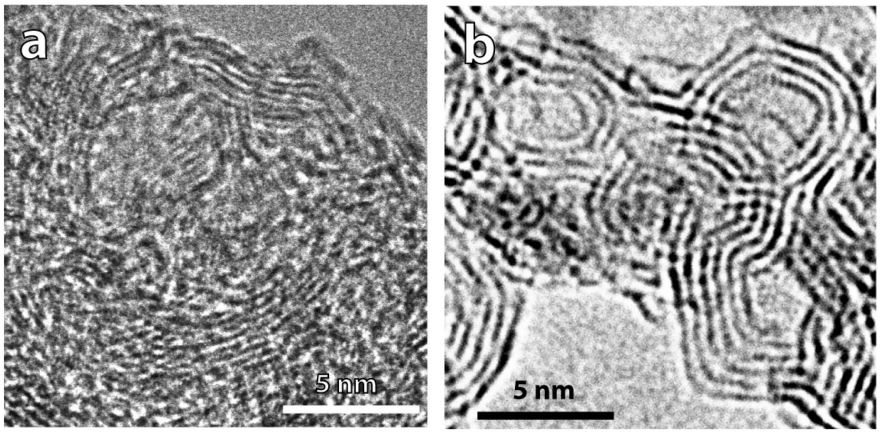

Fig. 6. Onion-like structure observed in Kainsaz IOM (a) and in heating experiments of nanodiamonds (b).

Table 2. Average values for structural parameters of Kainsaz IOM, the same values for Orgueil, Murchison, and Tagish Lake IOM are given for comparison.

	L (nm)	Single layers (%)	La (nm)	Lc (nm)	N	D (nm)
Kainsaz (CO3)	0.5	60	0.38	0.57	2.5	0.40
Orgueil (CI)	0.58	75	0.38	0.61	2.3	0.47
Murchison (CM)	0.55	65	0.30	0.59	2.2	0.49
Tagish Lake (C2)	0.61	58	0.31	0.58	2.2	0.46

L = Length of the layers; La = Diameter of coherent domains; Lc = Height of the coherent domains; N = Number of stacked layers per coherent domain; D = Interlayer spacing.

components in the IOM of carbonaceous chondrites: 1) free organic matter (FOM) that are extracted by usual solvents; 2) thermally labile organic matter (LOM), insoluble macromolecular material that can be cracked upon thermal stress (for instance pyrolysis); and 3) refractory organic matter (ROM) poorly affected by all these treatments. The most thermally metamorphosed parent bodies should have lost LOM and FOM, leaving only ROM. $\delta^{13}C$ values of CO3, which mainly reflect the isotopic composition of CO3 IOM, are in agreement with this scheme (Greenwood and Franchi 2004). The IOM of CO3 should be the residue of thermally processed organic matter precursor common to all carbonaceous chondrites.

This process is also consistent with the loss of radicals, whose abundance is two orders of magnitude lower than in CI and CM carbonaceous chondrites. As a matter of fact, in the case of coals, Mrozowski (1988) showed by extrapolation of kinetic studies that exposure to thermal stress over million years at temperatures in the range 300–400 °C could be sufficient to induce a significant decrease in radical concentration. Even if coals and meteoritic IOM have quite different origins and structures, close activation energies for radical annihilation should be expected for both types of materials, since both of them contain similar chemical bonds. Therefore a thermal stress on the parent body of Kainsaz at the maximum suspected temperatures of 330–350 °C (Semjonova et al. 1982; Bonal et al. 2007) over a few million years could account for the low abundance of radicals as compared to the CI and CM meteorites. The lack of heteroelements in the radicals in Kainsaz IOM is also consistent with the hypothesis of exposure to thermal stress, since studies on the thermal maturation of coals showed that the latter was accompanied by a loss of oxygen and a decrease of the *g* values, which approached the free electron value (Conard 1984). The lack of diradicaloid species in Kainsaz, which was the fingerprint of CM and CI meteorites may be attributed either to a particular instability of these species upon thermal stress, or by a slight increase of the size of their aromatic moieties resulting itself from the thermal stress. In the latter case, quantum calculations actually showed that when the aromatic moieties contained more than approximately 40 carbon atoms, the triplet state of the diradicaloids became the ground state (Binet et al. 2004a), so that the magnetism should then be almost temperature-independent. However, different synthetic processes and different precursors than CI and CM carbonaceous chondrites cannot be definitively ruled out to account for the lack of diradicaloids.

Effect of Thermal Stress on Structure of IOM

Raman spectra of Kainsaz IOM (Bonal et al. 2007) compared with those of Orgueil and Murchison IOM clearly show that the former is much more organized, exhibiting two not too broad "G" and "D" peaks representing the characteristics of the graphitic structures (breathing mode of

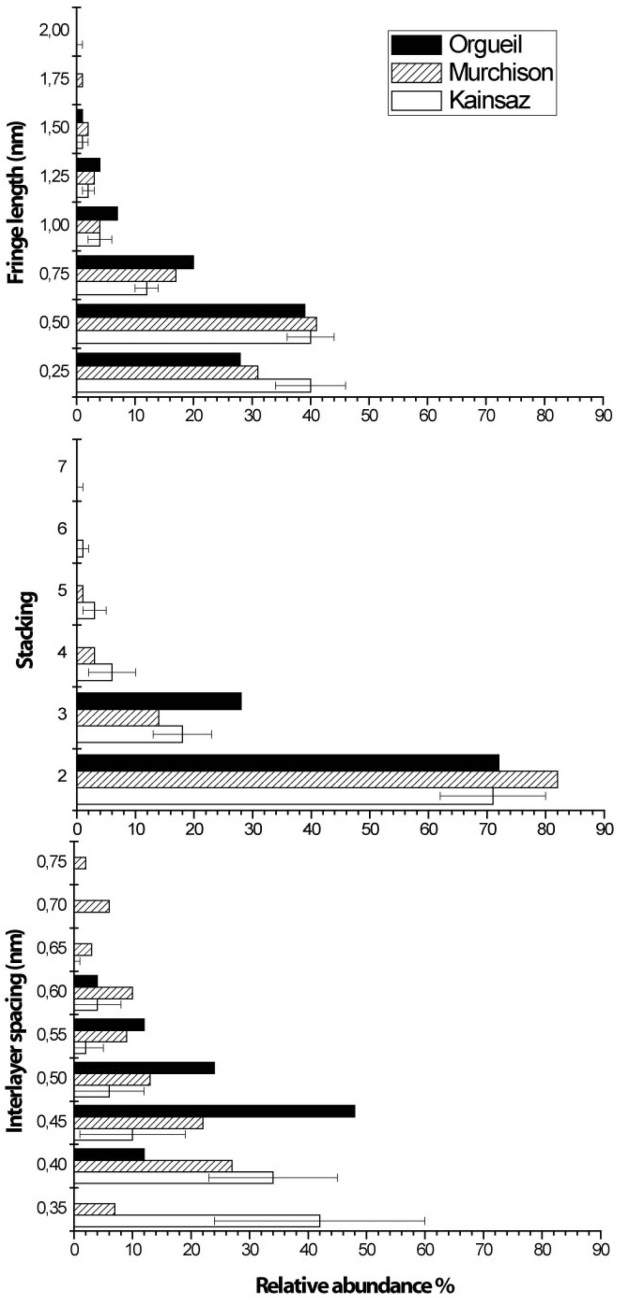

Fig. 7. Distributions of fringe length, number of stacked layers, and interlayer spacing in Kainsaz IOM. These data were obtained from the average of data from image analysis of 12 different areas in poorly organized carbon. Error bars indicate the variations between those areas. The same distributions for Orgueil and Murchison IOM (from Derenne et al. 2005) are also given.

the condensed polyaromatic rings and defect bands, respectively), whereas Orgueil and Murchison give much broader bands, especially as far as the defect band is concerned (Quirico et al. 2005). This is the consequence of the poorly organized structure of CI and CM IOM compared to that of CO or CV. Raman microspectrometry gives mean structural data at the μm^3 scale. Consequently, Raman spectra averaged the structural and microtextural heterogeneity evidenced by HRTEM and appeared as the superimposition of spectra of graphitized areas and of disordered IOM. The classifications, based on the maturity degree obtained by these two independent methods, appear to be in a good agreement. Orgueil and Murchison are essentially made of disordered IOM. In contrast, as far as Kainsaz is concerned, HRTEM detects a slightly higher maturity for the disordered IOM, but the ordered carbons represent about a third of this object. Such Raman and TEM data well agree with the H/C and pyrolysis experiments.

The main difference in the structural behavior of IOM from Kainsaz and more primitive carbonaceous chondrites is that interspacing between aromatic layers is smaller in Kainsaz IOM. This should reflect the process that takes place in the IOM while it is subjected to thermal stress. As it is observed in terrestrial kerogens (Durand 1980), IOM loses oxygen and nitrogen functions along with hydrogen, leading to a decrease of the H/C ratio. This is consistent with elemental analysis and pyrolysis data, which do not reveal neither highly substituted nor heteroelements-containing compounds depleted in heteroelements of the radicals. Then, aromatic units are reoriented to share common directions and interlayer spacing decreases (the aromatic units become closer) thanks to the loss of side and functional groups, leading to an increase of the number of stacked layers and a decrease of the single (i.e., non-stacked) layer proportion. All these tendencies are in a good agreement with the HRTEM observation: occurrence of a noticeable amount of ordered carbons, including graphitized particles, noticeable structural improvement of the disordered but main fraction of the IOM. It is likely that aromatization would occur if thermal stress increased as observed in Precambrian organic matter (Jehlicka and Rouzaud 1993). As a result, the structural organization is improved (larger, more planar, and better stacked layers). The occurrence of graphitized particles is a major argument for an important thermal stress. However, one might question this graphite could be presolar graphite grains or graphite formed on the parent body. The observation of regions with only partially graphitized (see Fig. 4b) areas with a lot of structural defects (i.e., responsible for fringe interruptions) should indicate progressive thermal processing of organic material, allowing graphite occurrence in some places. Moreover, in their attempt to determine abundances of presolar grains by noble gas release pattern, Huss et al. (2002) found no presolar graphite in Kainsaz. Thus the graphite we describe should be formed on the parent body due to thermal maturation of Kainsaz IOM.

In some areas, tiny nanoporous structures are observed; their pore walls are made of several concentric layers giving birth to onion-like structures (Fig. 6). Such structures can be attributed to thermal decomposition of nanodiamonds, as recently shown by Le Guillou and Rouzaud (2007). Submitted to a heat treatment up to 1000 °C for 15 min and

under inert atmosphere, industrial nanodiamonds progressively transformed into onion-like nanostructures (Le Guillou and Rouzaud 2007). This should be in agreement with the thermal metamorphism event that affected the parent body of Kainsaz IOM. Unfortunately, up to now, we were not able to observe neither nanodiamonds nor association between nanodiamonds and onion-like structures showing direct evidence of destabilization of diamonds. This could be due to the very small amount of nanodiamonds in Kainsaz, between 61 ppm (Newton et al. 1992a) to 873 ± 304 ppm (Huss et al. 2002). Consequently, the probability of detecting them on the TEM grids is very low.

Do Orgueil, Murchison and Kainsaz Have a Common Organic Precursor?

Our results clearly show that Kainsaz IOM is rather different from IOM of more primitive carbonaceous chondrites. Orgueil and Murchison IOMs are quite homogeneously constituted of poorly organized carbon, in contrast to Kainsaz IOM, where poorly organized carbon is associated with graphitic structures with micro- or meso-porous microtextures, partially graphitized particles and graphite. Two hypotheses can be proposed: 1) Kainsaz parent body had accreted similar IOM as CI and CM carbonaceous chondrites and had afterward experienced higher temperature, leading to a thermally induced maturation of IOM (Bonal et al. 2007), or 2) Kainsaz has accreted different IOM from a different region of the solar system and/or which would have experienced different stress prior to accretion (Huss et al. 2002).

The first hypothesis is supported by isotopic studies on CO carbonaceous chondrites. $^{13}C/^{12}C$ ratios lead Alexander et al. (1998) to conclude that all carbonaceous chondrites had accreted similar organic material, which had experienced various hydrous and thermal alteration on parent bodies, inducing different evolutions and metamorphic grades. Moreover, several mineralogical arguments prove that CO chondrites have experienced thermal metamorphism. Nevertheless, it is not possible to exclude that IOM was thermally processed before parent body accretion. Indeed, even if a common precursor exists, CI, CM, and CO chondrites condensed at different distances to the Sun and so at different temperatures. Then IOM of CO chondrites should have been exposed to a hotter gas than CI and CM chondrites, resulting in thermal stress experienced before parent body accretion. Therefore, as the parent body also experienced thermal stress, it would not be possible to distinguish if the IOM was processed before or after the parent body accretion. Moreover, in the second hypothesis, IOM could also be a mixing between poorly organized and graphitic-like carbon. Indeed, carbonaceous chondrites are known to be breccias due to the condensation process leading to the formation of their parent bodies. It should be possible that IOM in Kainsaz is the result of the association of two components that have experienced two different thermal stresses; these two components might then be related to the two phases "Q" in carbonaceous chondrites based on the noble-gas release pattern (Busemann et al. 2000).

If the organic precursor is common to CI, CM, and CO, then the thermal event is responsible for the increase in heterogeneity. The occurrence of intermediate phases (partially graphitized carbon particles) is clear evidence of an increasing graphitization with the metamorphism recorded on the parent body. Indeed, such heterogeneities were already systematically observed for graphitization either in natural environments under the metamorphism effect (Jehlicka and Rouzaud 1993), or during pyrolysis under pressure experiments (Beyssac et al. 2002). Because mineral matrix was mainly destroyed by the chemical treatment to extract the IOM, it is not possible to assume if a mineral interaction could also influence graphitization and enhance it in some places rather than others.

CONCLUSION

Our study shows that thermal stress has induced noticeable changes into the IOM of Kainsaz, compared to that of CI and CM. Thermally labile component is absent, leaving a more refractory fraction that does not release a high amount of products upon pyrolysis. The thermal stress is likely responsible for the loss of the typical fingerprint of CI and CM IOM concerning the radical distribution. Actually, EPR reveals that Kainsaz IOM contains fewer radicals compared to Orgueil, Murchison, and Tagish Lake, and that there are no diradicaloids. Furthermore, the radicals in Kainsaz IOM do not contain any heteroelement, in contrast with those of CI and CM IOMs. As seen by HRTEM, the multiscale organization of Kainsaz IOM is also different from that of CI and CM. It is very heterogeneous and contains disordered graphitic carbons with porous microtextures, partially graphitized and graphite-like lamellae. Graphitization is likely a consequence of thermal stress experienced by the IOM. Moreover, the few onion-like graphitic nanostructures could be due to thermal treatment of nanodiamonds. Poorly organized carbon structure is quite similar to that of CI and CM, except that aromatic layers are better stacked, likely due to loss of functional groups and branched aliphatic side chains.

Data obtained by the independent techniques used in this work to study the Kainsaz IOM structure are in a good agreement and are in favour of a higher degree of maturity of Kainsaz in comparison with Orgueil and Murchison. This higher degree of maturity might be the result of the thermal metamorphism on the parent body and/or a thermal stress experienced in the solar nebula gaseous phase prior accretion.

Acknowledgments—L. R. thanks Anne Salaün and Patrick Richon for helpful discussions on the statistical data analysis and helpful comments. Hikaru Yabuta and an anonymous referee are thanked for their constructive comments and suggestions. This is IPGP contribution no. 2267.

Editorial Handling—Dr. Scott Sandford

REFERENCES

Aléon J., Robert F., Duprat J., and Derenne S. 2005. Extreme oxygen isotope ratios in the early solar system. *Nature* 437:385–388.

Alexander C. M. O'D., Russel S. S., Arden J. W., Ash R. D., Grady M. M., and Pillinger C. T. 1998. The origin of chondritic macromolecular organic matter: A carbon and nitrogen isotope study. *Meteoritics & Planetary Science* 33:603–622.

Barklie R. C. 2001. Characterisation of defects in amorphous carbon by electron paramagnetic resonance. *Diamond and Related Materials* 10:174–181.

Beyssac O., Rouzaud J.-N., Goffe B., Brunet F., and Chopin C. 2002. Graphitization in a high-pressure, low-temperature metamorphic gradient: A Raman microspectrometry and HRTEM study. *Contribution in Mineralogy and Petrology* 143:19–31.

Binet L., Gourier D., Derenne S., and Robert F. 2002. Heterogeneous distribution of paramagnetic radicals in insoluble organic matter from the Orgueil and Murchison meteorites. *Geochimica et Cosmochimica Acta* 66:4177–4186.

Binet L., Gourier D., Derenne S., Robert F., and Ciofini I. 2004a. Occurrence of abundant diradicaloid moieties in the insoluble organic matter from the Orgueil and Murchison meteorites: A fingerprint of its extraterrestrial origin? *Geochimica et Cosmochimica Acta* 68:881–891.

Binet L., Gourier D., Derenne S., Pizzarello S., and Becker L. 2004b. Diradicaloids in the insoluble organic matter from the Tagish Lake meteorite: Comparison with the Orgueil and Murchison meteorites. *Meteoritics & Planetary Science* 39:1649–1654.

Bonal L., Bourot-Denise M., Quirico E., Montagnac G., and Lewin E. 2007. Organic matter and metamorphic history of CO chondrites. *Geochimica et Cosmochimica Acta* 71:1605–1623.

Boulmier J.-L., Oberlin A., Rouzaud J.-N., and Villey M. 1982. Natural organic matters and carbonaceous materials: A preferential field of application for transmission electron microscopy. In *Scanning electron microscopy*, edited by O'Hare A. M. F. Chicago: Scanning Microscopy Int. pp. 1523–1538.

Busemann H., Baur H., and Wieler R. 2000. Primordial noble gases in "phase Q" in carbonaceous and ordinary chondrites studied by closed-system stepped etching. *Meteoritics & Planetary Science* 35:949–973.

Chizmadia L. J., Rubin A. E., and Wasson J. T. 2002. Mineralogy and petrology of amoeboid olivine inclusions in CO3 chondrites: Relationship to parent-body aqueous alteration. *Meteoritics & Planetary Science* 37:1781–1796.

Cody G. D. and Alexander C. M. O'D. 2005. NMR studies of chemical and structural variation of insoluble organic matter from different carbonaceous chondrite groups. *Geochimica et Cosmochimica Acta* 69:1085–1097.

Conard J. 1984. EPR in fossil carbonaceous materials. In *Magnetic resonance: Introduction, advanced topics and applications to fossil energy*, edited by Petrarkis I. and Fraissard J. P. D. Dordrecht: Reidel Publishing Company. pp. 441–459.

Daulton T. L., Eisenhour D. D., Bernatowicz T. J., Lewis R. S., and Buseck P. R. 1996. Genesis of presolar diamonds: Comparative high-resolution transmission electron microscopy study of meteoritic and terrestrial nanodiamonds. *Geochimica et Cosmochimica Acta* 60:4853–4872.

Derenne S., Rouzaud J.-N., Clinard C., and Robert F. 2005. The size discontinuity between interstellar and chondritic aromatic structures: A high-resolution transmission electron microscopy study. *Geochimica et Cosmochimica Acta* 69: 3911–3917.

Durand B. 1980. *Kerogen: Insoluble organic matter from sedimentary rocks.* Editions Technip. 519 p.

Galvez A., Herlin-Boime N., Reynaud C., Clinard C., and Rouzaud J.-N. 2002. Carbon nanoparticles from laser pyrolysis. *Carbon* 40:2775–2789.

Gardinier A., Derenne S., Robert F., Behar F., Largeau C., and Maquet J. 2000. Solid state ^{13}C NMR of the insoluble organic matter of the Orgueil and Murchison meteorites: Quantitative study. *Earth and Planetary Science Letters* 184:9–21.

Garvie L. A. J. and Buseck P. R. 2004. Nanosized carbon-rich grains in carbonaceous chondrite meteorites. *Earth and Planetary Science Letters* 224:431–439.

Gourier D., Binet L., Skrzypczak A., Derenne S., and Robert F. 2004. Search for EPR markers of the history and origin of the insoluble organic matter in extraterrestrial and terrestrial rocks. *Spectrochimica Acta Part A* 60:1349–1357.

Greenwood R. C. and Franchi I. A. 2004. Alteration and metamorphism of CO3 chondrites: Evidence from oxygen and carbon isotopes. *Meteoritics & Planetary Science* 39:1823–1838.

Harris P. J. F., Vis R. D., and Heymann D. 2000. Fullerene-like carbon nanostructures in the Allende meteorite. *Earth and Planetary Science Letters* 183:355–359.

Hayatsu R., Winans R. E., Scott R. G., McBeth R. L., Moore L. P., and Studier M. H. 1980. Phenolic ethers in the organic polymer of the Murchison meteorite. *Science* 207:1202–1204.

Huss G. R., Meshik A. P., Hohenberg C. M., and Smith J. B. 2002. Relationships among chondrite groups as inferred from presolar grain abundances (abstract #1910). 33rd Lunar and Planetary Science Conference. CD-ROM.

Jehlicka J. and Rouzaud J.-N. 1993. Precambrian organic matter. In *Bitumens and metallogeny* edited by Parnell J., Kucha H., and Landais P. Berlin-Heidelberg: Springer-Verlag. pp. 53–60.

Keller L. P., Hony S., Bradley J. P., Molster F. J., Waters L. B. F. M., Bouwman J., de Koter A., Brownlee D. E., Flynn G. J., Henning T., and Mutschke H. 2002. Identification of iron sulphide grains in protoplanetary disks. *Nature* 417:148–150.

Le Guillou C., Brunet F., Irifune T., Ohfuji H., and Rouzaud J.-N. 2007. Nanodiamond nucleation below 2273 K at 15 GPa from carbons with different structural organizations. *Carbon* 45:636–648.

Le Guillou C. and Rouzaud J. N. 2007. Nanodiamonds graphitization under temperature: Implications on their evolution during chondrites parent body metamorphism (abstract #1578). 38th Lunar and Planetary Science Conference. CD-ROM.

Levy R. L., Grayson M. A., and Wolf G. J. 1973. The organic analysis of the Murchison meteorite. *Geochimica et Cosmochimica Acta* 37:467–483.

McSween H. Y. 1977. Carbonaceous chondrites of the Ornans type: A metamorphic sequence. *Geochimica et Cosmochimica Acta* 41:477–491.

Mrozowski S. 1988. ESR studies of carbonization and coalification processes part II: Biological materials. *Carbon* 26:531–541.

Murae T. 1995. Characterization of extraterrestrial high molecular weight organic matter by pyrolysis-gas chromatography/mass spectrometry. *Journal of Analytical and Applied Pyrolysis* 32: 65–73.

Nakamura K., Zolensky M. E., Tomita S., Nakashima S., and Tomeoka K. 2002. Hollow organic globules in the Tagish Lake meteorite as possible products of primitive organic reactions. *International Journal of Astrobiology* 1:179–189.

Nakamura-Messenger K., Messenger S., Keller L. P., Clemett S. J., and Zolensky M. E. 2006. Organic globules in the Tagish Lake meteorite: remnants of the protosolar disk. *Science* 314:1439–1442.

Newton J., Arden J. W., and Pillinger C. T. 1992a. Metamorphism of CO3 chondrites: A carbon and nitrogen isotope study. *Meteoritics* 27:267–268.

Newton J., Arden J. W., and Pillinger C. T. 1992b. Carbon and nitrogen isotope studies of a suite of type CO3 carbonaceous chondrites (abstract). 23rd Lunar and Planetary Science Conference. p. 985.

Papoular R., Conard J., Guillois O., Nenner I., Reynaud C., and Rouzaud J.-N. 1996. A comparison of solid-state carbonaceous models of cosmic dust. *Astronomy and Astrophysics* 315:222–236.

Pizzarello S., Cooper G. W., and Flynn G. J. 2006. The nature and distribution of the organic material in carbonaceous chondrites and interplanetary dust particles. In *Meteorites and the early solar system II*, edited by Lauretta D. and McSween H. Y. Jr. Tucson: The University of Arizona Press. pp. 625–651.

Quirico E., Borg J., Raynal P.-I., Montagnac G., and d'Hendecourt L. 2005. A micro-Raman survey of 10 IDPs and 6 carbonaceous chondrites. *Planetary & Space Science* 53:1443–1448.

Remusat L., Derenne S., Robert F., and Knicker H. 2005a. New pyrolytic and spectroscopic data on Orgueil and Murchison insoluble organic matter: A different origin than soluble? *Geochimica et Cosmochimica Acta* 69:3919–3932.

Remusat L., Derenne S., and Robert F. 2005b. New insight on aliphatic linkages in the macromolecular organic fraction of Orgueil and Murchison meteorites through ruthenium tetroxide oxidation. *Geochimica et Cosmochimica Acta* 69:4377–4386.

Retcofsky H. L., Stark J. M., and Friedel R. A. 1968. Electron spin resonance in American coals. *Analytical Chemistry* 40:1699–1704.

Rouzaud J.-N. and Oberlin A. 1990. The characterization of coals and cokes by transmission electron microscopy. In *Advanced methodologies in coal characterization*, vol. 17, edited by Charcosset H. and Nickel-Pepin-Donat B. Amsterdam: Elsevier. pp. 311–355.

Rouzaud J.-N. and Clinard C. 2002. Quantitative high resolution transmission electron microscopy: A promising tool for carbon materials characterization. *Fuel Processing Technology* 77–78: 229–235.

Scott E. R. D. and Jones R. H. 1990. Disentangling nebular and asteroidal features of CO3 carbonaceous chondrite meteorites. *Geochimica et Cosmochimica Acta* 54:2485–2502.

Scott E. R. D. and Krot A. N. 2003. Chondrites and their components. In *Meteorites, comets, and planets*, edited by Davis A. M. Treatise of geochemistry, vol. 1. Amsterdam: Elsevier. pp. 144–200.

Semjonova L. F., Karyakin A. V., Fisenko A. V., Sorokina T. S., Efimova N. F., and Lavrukhina A. K. 1982. Investigation of the extractable organic constituent of the Kainsaz carbonaceous chondrite. 13th Lunar and Planetary Science Conference. pp. 708–709.

Sephton M. A., Pillinger C. T., and Gilmour I. 2000. Aromatic moieties in meteoritic macromolecular materials: Analysis by hydrous pyrolysis and $\delta^{13}C$ of individual compounds. *Geochimica et Cosmochimica Acta* 64:321–328.

Sephton M. A., Verchovsky A. B., Bland P. A., Gilmour I., Grady M. M., and Wright I. P. 2003. Investigating the variations in carbon and nitrogen isotopes in carbonaceous chondrites. *Geochimica et Cosmochimica Acta* 67:2093–2108.

Sephton M. A., Love G. D., Watson J. S., Verchovsky A. B., Wright I. P., Snape C. E., and Gilmour I. 2004. Hydropyrolysis of insoluble carbonaceous matter in the Murchison meteorite: New insights into the macromolecular structure. *Geochimica et Cosmochimica Acta* 68:1385–1393.

Shimoyama A. 1997. Complex organics in meteorites. *Advances in Space Research* 19:1045–1052.

Westall F., De Vries S. T., Nijman W., Rouchon V., Orberger B., Pearson V. K., Watson J. S., Verchovsky A. B., Wright I. P., Rouzaud J.-N., Marchesini D., and Anne S. 2006. The 3.466 Ga "Kitty's Gap Chert," an early Archean microbial ecosystem. In *Processes on the early Earth*, edited by Reimold W. U. and Gibson R. L. GSA Special Paper 405. pp. 105–131.